



Vaccination and Quarantine Effect on COVID-19 Transmission Dynamics Incorporating Chinese-Spring-Festival Travel Rush: Modeling and Simulations

Yukun Zou^{1,2} · Wei Yang¹  · Junjie Lai^{1,2} · Jiawen Hou^{1,2} · Wei Lin^{1,3,4}

Received: 18 May 2021 / Accepted: 20 October 2021 / Published online: 10 January 2022
© The Author(s), under exclusive licence to Society for Mathematical Biology 2022

Abstract

The COVID-19 pandemic has adversely affected the entire world. The effective implementation of vaccination strategy is critical to prevent the resurgence of the pandemic, especially during large-scale population migration. We establish a multiple patch coupled model based on the transportation network among the 31 provinces in China, under the combined strategies of vaccination and quarantine during large-scale population migration. Based on the model, we derive a critical quarantine rate to control the pandemic transmission and a vaccination rate to achieve herd immunity. Furthermore, we evaluate the influence of passenger flow on the effective reproduction number during the Chinese-Spring-Festival travel rush. Meanwhile, the spread of the COVID-19 pandemic is investigated for different control strategies, viz. global control and local control. The impact of vaccine-related parameters, such as the number, the effectiveness and the immunity period of vaccine, are explored. It is believed that the articulated models as well as the presented simulation results could be beneficial to design of feasible strategies for preventing COVID-19 transmission during the Chinese-Spring-Festival travel rush or the other future events involving large-scale population migration.

Keywords Multiple patch coupled model · Transportation network · Vaccination · Basic reproduction number · Large-scale migration

1 Introduction

Coronavirus disease 2019 (COVID-19) pandemic has spread across the whole world since December 2019 (Li et al. 2020; Hou et al. 2021), which has severely affected public health and economics (Guan et al. 2020; Jacobsen 2020; Brown et al. 2020). Due to various prevention and control measures, the pandemic is being alleviated

(Sheikh et al. 2020; Li et al. 2020). Nevertheless, the risk of periodic pandemic still requires adequate attention.

Population migration between cities plays an important role in the pandemic transmission (Wesolowski et al. 2012; Auger and Moussaoui 2021), and the coupling of population flows between different cities is worth investigating. A traffic-network-driven infectious disease model is proposed and applied to investigate the worldwide 2009 H1N1 influenza and 2003 SARS pandemic transmission (Brockmann and Helbing 2013), which is later used to identify the spatial origin of spreading process (Pan 2018). Analyses of the topology and evolution population flow network help understand the influence on the early dynamics of COVID-19 transmission (Liu et al. 2021). During the Chinese-Spring-Festival (CSF) travel rush, the spatial transmission model is used to reveal the transmission mechanism of COVID-19 between or among cities (Mu et al. 2020). Similarly, a population movement model based on spatial networks is considered in the spread of pandemic in Indi (Pujari and Shekatkar 2020). In metropolis of the USA, the impact of population flow on the pandemic transmission is characterized by the population migration cell model (Shen et al. 2021) and the dynamic cabin model (Chang et al. 2021).

Before the availability of effective vaccine, non-pharmaceutical interventions (NPIs) were taken into account controlling the pandemic spread (Perkins and España 2020; Lai et al. 2020; Fang et al. 2020). In terms of local intervention, the lockdown strategy of Wuhan during a concentrated outbreak of COVID-19 was effective (Lau et al. 2020). Meanwhile, with respect to global interventions, quarantine, and travel restrictions were the main control strategies during the outbreak (Fang et al. 2020; Kissler et al. 2020; Kraemer et al. 2020; Zhang et al. 2020). After that the pandemic was alleviated, decentralized population flow was adopted to sustain economic activities (Nishi et al. 2020), and similar policies were formulated in France to reopen schools (Di Domenico et al. 2021).

Since January 2021, more than ten types of vaccine against the COVID-19 pathogen SARS-CoV-2 have been fully or limitedly approved and used in clinics (Jeyanathan et al. 2020). Vaccination to obtain immunity is the most fundamental way to prevent the spread of infectious diseases (Lipsitch and Dean 2020). In the concurrent case of COVID-19 pandemic and influenza, it is especially important to increase the vaccination rate (Gostin and Salmon 2020; Amato et al. 2020). The public's acceptance of vaccine largely depends on its effectiveness and safety (Kim et al. 2021). The Centers for Disease Control and Prevention (CDC) has evaluated the effectiveness of vaccines in preventing infection of medical workers in the USA (Thompson et al. 2021). Due to the scarcity of vaccines, priority groups for vaccination have been discussed (Medlock and Galvani 2009; Bubar et al. 2021). Moreover, the combination of vaccination and social distance control can result in better pandemic prevention (Huang et al. 2021; Gallagher et al. 2020). Practically, policy makers hope to achieve herd immunity by vaccination (DeRoo et al. 2020), namely, the basic reproduction number \mathcal{R}_0 is less than 1, to completely restore normal social order and economic activities, which may take a long time for COVID-19. Therefore, together with NPIs, the vaccination strategy is worthy of further exploration.

Motivated by the promotion of vaccination strategy and the large-scale population migration during the CSF travel rush, we establish a multiple patch coupled model to explore the impact of vaccination and NPIs on the COVID-19 transmission dynamics. This paper is structured as flows. In Sect. 2, we formulate a coupled compartment model based on the real travel network of China, incorporating NPIs and vaccination strategies. In Sect. 3, we investigate several critical model parameters to mimic various scenarios, including the vaccination rate, the effectiveness and the immunity period of vaccines and the passage flow during the CSF travel rush. Finally, we summarize and give some suggestions on the prevention of COVID-19 transmission in China.

2 Mathematical Model

2.1 Basic Model Based on Transportation Network

We first construct a basic model in a multiple patch setting based on transportation network among 31 provinces (including 27 provinces, municipalities and 4 directed cities) in China. In each patch, namely within a single province, we use an SEIR model, which is coupled with the other patches (provinces) by transportation network. Here, we simplify the flow in and out of each patch at fixed time everyday, which results in a pulse input and output of the system. The flow diagram of the SEIR model within each patch, the movement between every two patches and the corresponding SEI model during the transportation cabin, is depicted in Fig. 1.

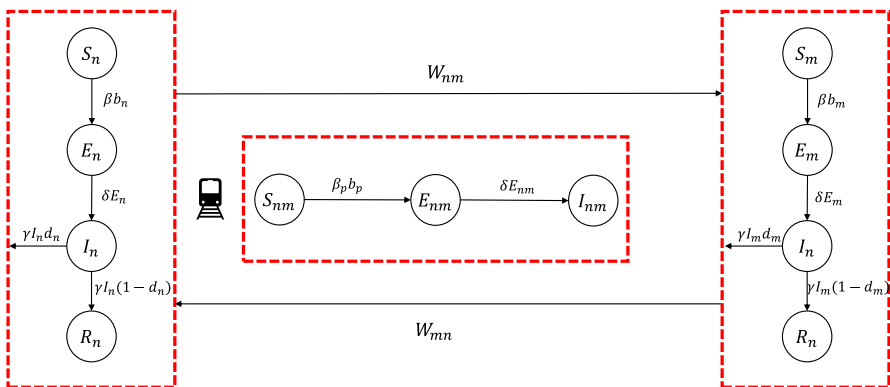


Fig. 1 A flow diagram of the SEIR model within each patch and the SEI model during transportation, where $b_n = I_n S_n / N_n + p_1 E_n S_n / N_n$, $b_m = I_m S_m / N_m + p_1 E_m S_m / N_m$, and $b_p = I_{nm} S_{nm} / N_{nm} + p_1 E_{nm} S_{nm} / N_{nm}$

2.1.1 Model Formulation

The local transmission model within each patch takes the form

$$\begin{cases} \frac{dS_n}{dt} = -\beta I_n S_n / N_n - p_1 \beta E_n S_n / N_n, \\ \frac{dE_n}{dt} = \beta I_n S_n / N_n + p_1 \beta E_n S_n / N_n - \delta E_n, \\ \frac{dI_n}{dt} = \delta E_n - \gamma I_n, \\ \frac{dR_n}{dt} = \gamma I_n (1 - d_n), \end{cases} \tag{1}$$

where $n = 1, 2, \dots, 31$. The variables and the parameters in model (1) as well as in the following models are all listed in Table 1.

An $M \times M$ passenger flow matrix $W = \{W_{mn}\}$ is introduced to describe the daily passenger transportation among provinces, W_{mn} denotes the number of people from the m -th province to the n -th province. The following system quantifies the number of passengers in different states (S_n, E_n, I_n or R_n), traveling from the n -th province to the m -th province per day,

Table 1 Definitions of variables and parameters in the compartmental model (1) and (9)

Variables or parameters	Definition
S_n	The absolute number of susceptible individuals in the N -th city/province ($n = 1, \dots, 31$)
E_n	The absolute number of exposed individuals in the N -th city/province ($n = 1 \dots, 31$)
I_n	The absolute number of infectious individuals in the N -th city/province ($n = 1, \dots, 31$)
R_n	The absolute number of recovered or dead individuals in the N -th city/province ($n = 1, \dots, 31$)
N_n	The total population of the N -th country/region ($n = 1, \dots, 31$)
δ	The conversion rate from exposed to infectious
p_1	The relative infection rate of a susceptible individual by an exposed individual
p_2	The new infection cases quarantine rate
β	The probability of susceptible being infected by infectious
β_p	The infection rate of a travelling susceptible individual by an infected individual during transportation
γ	Mortality and recovery rate
N_{nv}	The amount of vaccine allocated to N -th province per day
v_e	Effectiveness of vaccines
ξ	The reciprocal of effective period of the vaccine
W_{nm}	Total number of people traveling from the m -th province to the n -th province ($n, m = 1, \dots, 31$)

$$\begin{cases} S_{nm} = S_n W_{nm} / N_n, \\ E_{nm} = E_n W_{nm} / N_n, \\ I_{nm} = I_n W_{nm} / N_n, \\ R_{nm} = R_n W_{nm} / N_n. \end{cases} \tag{2}$$

The population flow out of patch n by transportation (namely, people leaving by planes and trains) which contributes to the population within patch n is modeled by the system as

$$\begin{cases} S_n(t_k^1) = S_n(t_k^{1-}) - \sum_{m \neq n} S_{nm}(t_k^1), \\ E_n(t_k^1) = E_n(t_k^{1-}) - \sum_{m \neq n} E_{nm}(t_k^1), \\ I_n(t_k^1) = I_n(t_k^{1-}) - \sum_{m \neq n} I_{nm}(t_k^1), \\ R_n(t_k^1) = R_n(t_k^{1-}) - \sum_{m \neq n} R_{nm}(t_k^1), \\ t_k^1 = t_1 + kT, \quad k \in \mathbb{N}, \end{cases} \tag{3}$$

where the subscript nm means from the n -th patch to the m -th patch, t_1 is the taking time of the transportation, and T set as 1 day in the model is the period of population movement.

Similarly, the population flow into patch n by transportation (namely, people coming by planes and trains) contributes to the population within patch n , is modeled as

$$\begin{cases} S_n(t_k^2) = S_n(t_k^{2-}) + \sum_{m \neq n} S_{mn}(t_k^2), \\ E_n(t_k^2) = E_n(t_k^{2-}) + \sum_{m \neq n} E_{mn}(t_k^2), \\ I_n(t_k^2) = I_n(t_k^{2-}) + \sum_{m \neq n} I_{mn}(t_k^2), \\ R_n(t_k^2) = R_n(t_k^{2-}) + \sum_{m \neq n} R_{mn}(t_k^2), \\ t_k^2 = t_2 + kT, \quad k \in \mathbb{N}, \end{cases} \tag{4}$$

where t_2 is the landing time of the transportation from the m -th patch to the n -th patch.

Next, during the travel process, considered as a closed cabin, we use an SEI model with no recovered class as follows,

$$\begin{cases} \frac{dS_{nm}}{dt} = -\beta_p I_{nm} S_{nm} / N_{nm} - p_1 \beta_p E_{nm} S_{nm} / N_{nm}, \\ \frac{dE_{nm}}{dt} = \beta_p I_{nm} S_{nm} / N_{nm} + p_1 \beta_p E_{nm} S_{nm} / N_{nm} - \delta E_{nm}, \\ \frac{dI_{nm}}{dt} = \delta E_{nm}, \end{cases} \quad (5)$$

where β_p denotes the infectious rates during the transportation.

2.1.2 Basic Reproduction Number

Following the next generation matrix method (Van den Driessche and Watmough 2002) for compartmental models, we calculate the basic reproduction number \mathcal{R}_0 . Using the same notations as proposed in Van den Driessche and Watmough (2002), we write as

$$\mathcal{F} = \begin{pmatrix} \beta S_n I_n / N_n + p_1 \beta E_n S_n / N_n & & & \\ 0 & & & \\ 0 & & & \\ 0 & & & \end{pmatrix}, \mathcal{V} = \begin{pmatrix} \delta E_n & & & \\ -\delta E_n + \gamma I_n & & & \\ \beta I_n S_n / N_n - p_1 \beta E_n S_n / N_n & & & \\ \gamma I_n (1 - d_n) & & & \end{pmatrix}.$$

Setting the right-hand side of system (1) to zero, we always obtain the disease-free equilibrium $x_0 = (S_0, 0, 0, 0)$, with $S_0 = N_n$. Applying the Fréchet derivatives to \mathcal{F} and \mathcal{V} at x_0 , we, respectively, get

$$F = \begin{pmatrix} p_1 \beta & \beta \\ 0 & 0 \end{pmatrix}, \quad V = \begin{pmatrix} \delta & -0 \\ -\delta & \gamma \end{pmatrix}.$$

Then,

$$\mathcal{R}_0 = \rho(FV^{-1}) = \frac{\beta(p_1 \gamma + \delta)}{\gamma \delta}, \quad (6)$$

where $\rho(\cdot)$ represents the spectral radius of a given matrix.

Considering the vaccination on susceptibles, we assume the proportion of susceptibles getting vaccinated is α . Then $S_0^{\text{new}} = (1 - \alpha)S_0$. Letting

$$\mathcal{R}_0^{\text{new}} = \frac{(1 - \alpha)\beta(p_1 \gamma + \delta)}{\gamma \delta} < 1 \quad (7)$$

yields:

$$\alpha > 1 - \frac{\gamma \delta}{\beta(p_1 \gamma + \delta)} \triangleq \alpha_c. \quad (8)$$

This means that once the vaccination proportion is more than α_c , the herd immunity can be achieved.

2.2 Model with Quarantine and Vaccination

2.2.1 Model Formulation

Introducing strategies of quarantine and vaccination, the revised flow diagram of an SEIQRV model with transportation is shown in Fig. 2.

The model is governed by

$$\left\{ \begin{aligned} \frac{dS_n}{dt} &= -\beta I_n S_n / N_n - p_1 \beta E_n S_n / N_n - N_{nv} v_e + \xi V_n + \xi R_n, \\ \frac{dE_n}{dt} &= (\beta I_n S_n / N_n + p_1 \beta E_n S_n / N_n)(1 - p_2) - \delta E_n, \\ \frac{dI_n}{dt} &= \delta E_n(1 - p_2) - \gamma I_n, \\ \frac{dQ_n}{dt} &= (\beta I_n S_n / N_n + p_1 \beta E_n S_n / N_n + \delta E_n)p_2 - \gamma Q_n, \\ \frac{dR_n}{dt} &= \gamma I_n(1 - d_n) + \gamma Q_n - \xi R_n, \\ \frac{dV_n}{dt} &= N_{nv} v_e - \xi V_n, \end{aligned} \right. \tag{9}$$

where Q_n is the quarantine compartment, V_n is the vaccinated compartment, ξ represents the period of immunity, v_e represents the effectiveness of vaccine, p_2 represents the quarantine ratio, and N_{nv} is the number of vaccines provided everyday in the n -th patch. We assume that the vaccinated population would immediately gain immunity in the model.

To be clear, in system (9), the ratio of $N_{nv} v_e$ to the total population N_n , namely, $N_{nv} v_e / N_n$ is very small. Considering the total population of China and the distribution

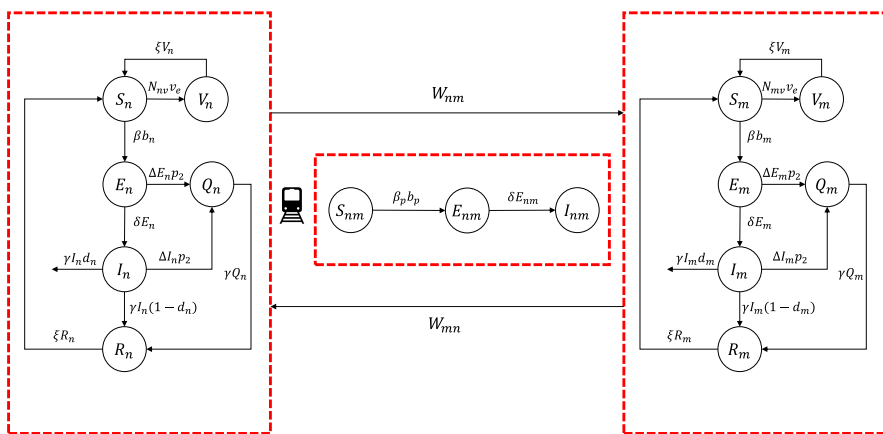


Fig. 2 A flow diagram of the SEIQRV model within each patch and the SEI model during transportation, where $b_n = I_n S_n / N_n + p_1 E_n S_n / N_n$, $b_m = I_m S_m / N_m + p_1 E_m S_n / N_m$, $\Delta E_n = \beta I_n S_n / N_n + p_1 \beta E_n S_n / N_n$, and $\Delta I_n = \delta E_n$

in each province, the ratio is about 10^{-4} . Moreover, we assume that the vaccinated population only gain certain immunity period, characterized by the parameter ξ . Therefore, in the simulated time span, there will be no negative solutions according to the parameter settings.

The passenger flow leaving the patch n takes the form as

$$\left\{ \begin{array}{l} S_n(t_k^1) = S_n(t_k^{1-}) - \sum_{m \neq n} S_{nm}(t_k^1), \\ E_n(t_k^1) = E_n(t_k^{1-}) - \sum_{m \neq n} E_{nm}(t_k^1), \\ I_n(t_k^1) = I_n(t_k^{1-}) - \sum_{m \neq n} I_{nm}(t_k^1), \\ R_n(t_k^1) = R_n(t_k^{1-}) - \sum_{m \neq n} R_{nm}(t_k^1), \\ V_n(t_k^1) = V_n(t_k^{1-}) - \sum_{m \neq n} V_{nm}(t_k^1), \\ t_k^1 = t_1 + KT, \quad K \in \mathbb{N}, \end{array} \right. \tag{10}$$

and the flow coming into the patch n is given by

$$\left\{ \begin{array}{l} S_n(t_k^2) = S_n(t_k^{2-}) + \sum_{m \neq n} S_{mn}(t_k^2), \\ E_n(t_k^2) = E_n(t_k^{2-}) + \sum_{m \neq n} E_{mn}(t_k^2), \\ I_n(t_k^2) = I_n(t_k^{2-}) + \sum_{m \neq n} I_{mn}(t_k^2), \\ R_n(t_k^2) = R_n(t_k^{2-}) + \sum_{m \neq n} R_{mn}(t_k^2), \\ V_n(t_k^2) = V_n(t_k^{2-}) + \sum_{m \neq n} V_{mn}(t_k^2), \\ t_k^2 = t_2 + KT, \quad K \in \mathbb{N}. \end{array} \right. \tag{11}$$

The dynamical system during transportation still follows (5). Here, it is reasonably to assume that the vaccinated population would not lose immunity during the travel.

2.2.2 Basic Reproduction Number

Following the approach and the notations applied in Sect. 2.1.2, we calculate the basic reproduction number of the revised model (9). The disease-free equilibrium point of (9) is $x_0 = (0, 0, 0, 0, 0, V_0)$, where $S_0 + V_0 = N_n$ and $V_0 = N_{nv}v_e/\xi$. Thus, we have

$$\mathcal{F} = \begin{pmatrix} (1 - p_2)(\beta S_n I_n / N_n + p_1 \beta E_n S_n / N_n) \\ 0 \\ p_2(\beta S_n I_n / N_n + p_1 \beta E_n S_n / N_n) \\ 0 \\ 0 \\ 0 \end{pmatrix}, \mathcal{V} = \begin{pmatrix} \delta E_n \\ -\delta E_n(1 - p_2) + \gamma I_n \\ -\delta E_n(1 - p_2) + \gamma Q_n \\ \beta I_n S_n / N_n + p_1 \beta E_n S_n / N_n \\ + N_{nv} v_e + \xi V_n - \xi R_n \\ -\gamma I_n(1 - d_n) - \gamma Q_n + \xi R_n \\ -N_{nv} v_e + \xi V_n \end{pmatrix}.$$

These further give:

$$F = \begin{pmatrix} (1 - p_2)p_1\beta S_0/N_n & (1 - p_2)\beta S_0/N_n & 0 \\ 0 & 0 & 0 \\ p_1 p_2 \beta S_0 / N_n & p_2 \beta S_0 / N_n & 0 \end{pmatrix}, \quad V = \begin{pmatrix} \delta & 0 & 0 \\ -\delta & \gamma & 0 \\ -\delta p_2 & 0 & \gamma \end{pmatrix}.$$

Therefore, the basic reproduction number is given by

$$\begin{aligned} \mathcal{R}_0 &= \rho(FV^{-1}) \\ &= \frac{S_0\beta(\delta + \delta p_2^2 - 2\delta p_2 + \gamma p_1 - \gamma p_1 p_2)}{N_n \delta \gamma}. \end{aligned} \tag{12}$$

Remark 1 ompared with \mathcal{R}_0 derived in (6), S_0/N_n is not a constant here. This implies that \mathcal{R}_0 given in (12) is time-varying, and that it can be considered as an effective reproduction number.

3 Numerical Results

Based on the population flow data of China, we simulate the COVID-19 transmission with travel infection. The initial data are given by the reported cases on January 19, 2021, and the time span in simulations is taken as 300 days, including the CSF travel rush (from January 26 to March 9, 2021).

Because of the inaccessibility of population migration data in the transportation part, we generate a simulated population migration data based on Baidu migration (<http://qianxi.baidu.com/>), which contains the population migration rates between or among provinces. According to the number of migrant population given by the Chinese news reported (<https://baike.baidu.com/item/2021%E5%B9%B4%E6%98%A5%E8%BF%90/55222817?fr=aladdin>), we estimate the number of population immigration and emigration in each province every day, and calculate the migration data during the CSF travel rush. After the CSF travel rush, we reduce the passenger flow to 10% to mimic the normal daily population migration.

3.1 Herd Immunity

Considering the basic model (1), the condition to achieve herd immunity is given by (7). The parameters are listed in Table 1 and part of the default parameters values are

Table 2 Parameters settings in default scenario

Parameters	Default value	Reference
p_1	0.2	Ivorra et al. (2020)
p_2	0.4	Ivorra et al. (2020)
δ	1/5.5	Ivorra et al. (2020)
β	0.173	Calculated by (13)
β_p	$2 \cdot \beta$	Assumption
γ	1/14	Ivorra et al. (2020)
v_e	0.7	Ivorra et al. (2020)
ξ	1/50	Ivorra et al. (2020)
\mathcal{R}_0	2.6	Ivorra et al. (2020)

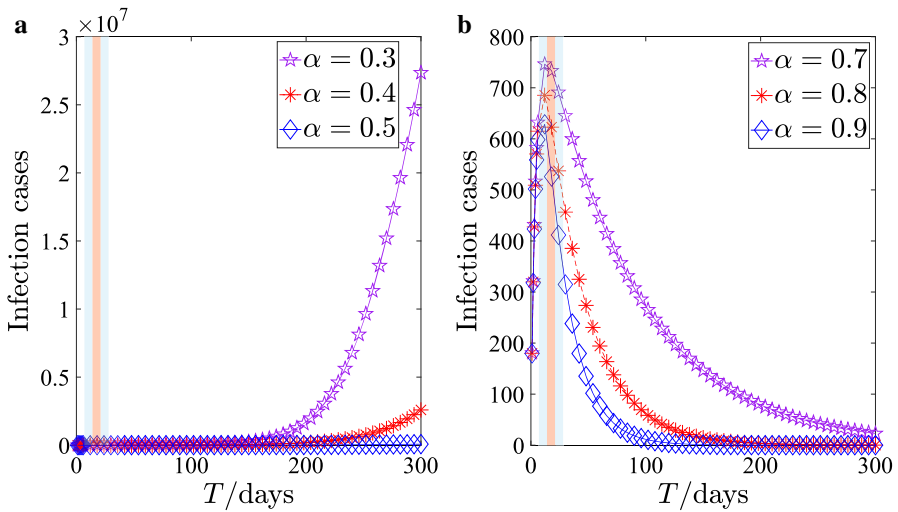


Fig. 3 Effect of the vaccinated proportion α on the pandemic transmission. The light (blue) shaded area represents the time interval during the Spring Festival travel rush and the dark (red) shaded area represent the Chinese Lunar Year. **a** $\alpha < \alpha_c$. **b** $\alpha > \alpha_c$

listed in Table 2. In the standard scenario, we set $\mathcal{R}_0 = 2.6$ (Ivorra et al. 2020), and calculate

$$\beta = \frac{\mathcal{R}_0 \gamma \delta}{p_1 \gamma + \delta} = 0.17219. \tag{13}$$

Under the parameter settings, the proportion α of the vaccinated susceptibles should be larger than $\alpha_c = 61.38\%$ to achieve herd immunity given by (8). The simulation results are shown in Fig. 3.

3.2 Sensitivity Analysis of \mathcal{R}_0 with Different Parameters

We present a sensitivity analysis of the value of \mathcal{R}_0 with variation of the parameters. All the parameters are changed in the ranges listed in Table 3. Each parameter is sampled 100 times within the given range. The simulation results are shown in Fig. 4.

3.3 Sensitivity Analysis of Infection Cases with Infection Rate β

The infection rate β will decline as the government implements control measures. We assume that β has a decay rate (D_r) and the new infection rate $\beta^{new} = \beta \cdot D_r$. The other parameters are only related to virus characteristics, which would not change much over time. We present a sensitivity analysis on β and the simulation results are shown in Fig. 5.

3.4 Quarantine Strategy

The quarantine strategy is taken to control the COVID-19 transmission in China, which plays great importance during the outbreak of the pandemic. From (12), letting $\mathcal{R}_0 < 1$, yields

Table 3 Parameters in different ranges

Parameters	Range	Sampling frequency
p_1	[0.1, 0.5]	100 times
p_2	[0.2, 0.6]	
δ	[0.1, 0.3]	
γ	[0.05, 0.1]	
β	[0.1, 0.3]	
ξ	[0.001, 1/30]	
v_e	[0.5, 0.9]	

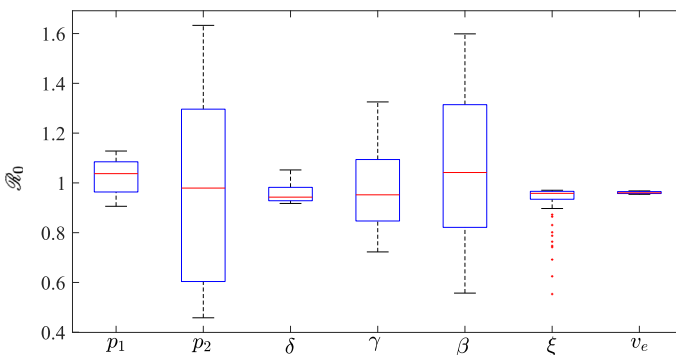


Fig. 4 Sensitivity of \mathcal{R}_0 with variation of the considered parameters

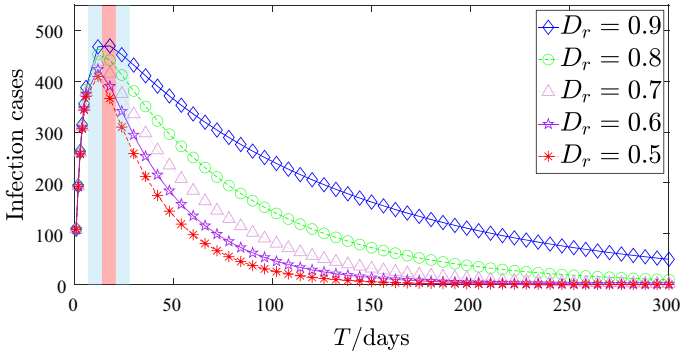


Fig. 5 Sensitivity of infection cases with β

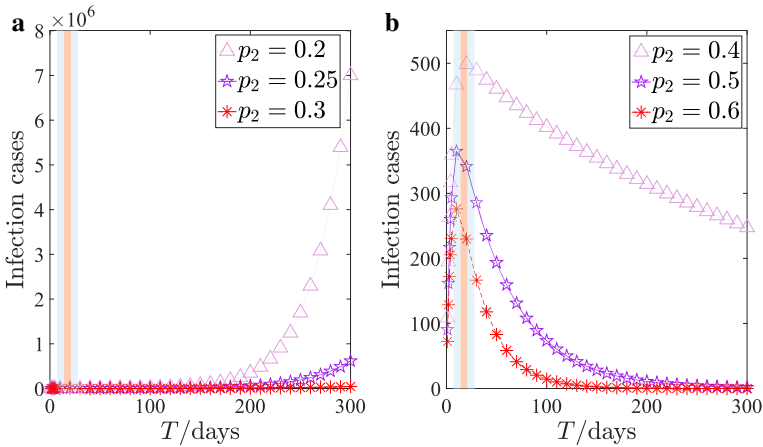


Fig. 6 The impact of p_2 on COVID-19 transmission. $p_2^c = 38.74\%$. **a** $p_2 < p_2^c$. **b** $p_2 > p_2^c$

$$p \geq 1 - \frac{\sqrt{S_0\beta(4N_n\delta^2 + S_0\beta\gamma p_1^2)} - S_0\beta\gamma^2 p_1}{2S_0\beta\delta\gamma} \triangleq p_2^c. \tag{14}$$

Under the setting of the parameter values specified in Table 2, we have $p_2^c \geq 38.74\%$. Figure 6 shows the impact of different values of p_2 on the epidemic transmission. To be clear, the curve seems to be close to zero because of the magnitude, but it keeps going up when $p_2 = 0.3$.

3.5 Relationship Between $\mathcal{R}_0(t)$ and Passenger Flow

From (12), we find that the effective reproduction number $\mathcal{R}_0(t)$ changes with passenger flow. Due to the daily population migration, the equilibrium point $x_0 = (S_0, 0, 0, 0, 0, 0, V_0)$ is different, where $S_0 + V_0 = N_n(t)$ and $N_n(t)$ is daily-varying.

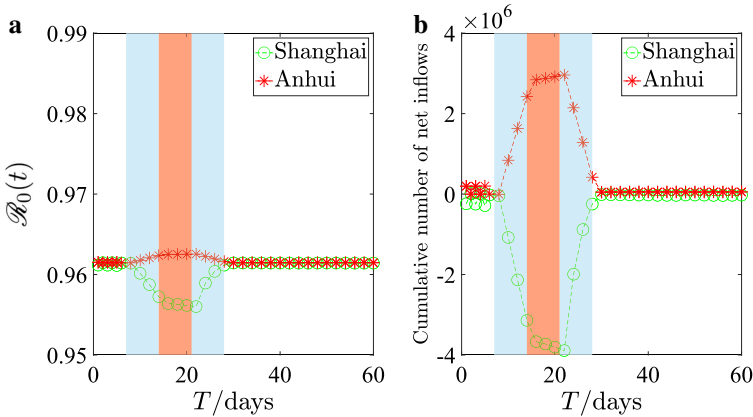


Fig. 7 Changes of \mathcal{R}_0 in Shanghai City and Anhui Province over time. **a** The red line represents the change of \mathcal{R}_0 in Shanghai over time, and the blue line represents the change of \mathcal{R}_0 over time in Anhui Province. **b** The red line represents the cumulative inflow of Shanghai, and the green line represents the cumulative inflow of Anhui Province

Here, we take Shanghai City (large-scale emigration) and Anhui Province (large-scale immigration) as examples to calculate the effective reproduction number $\mathcal{R}_0(t)$. Figure 7 shows the relationship of the effective reproduction number with passenger flow.

At the beginning of the CSF travel rush, $\mathcal{R}_0(t)$ of the provinces (e.g., Shanghai, Beijing, etc.) with large-scale emigration decreases with the increase of outgoing passenger flow. As for the provinces (e.g., Anhui, Henan, etc.) with large-scale immigration, $\mathcal{R}_0(t)$ increases correspondingly. At the rush of the CSF travel back to the city, the trend is opposite to those going out of the city. After the CSF rush, there is no obvious change in $\mathcal{R}_0(t)$.

3.6 Transition Matrix W Control: Global and Local

Now, we investigate the impact of passenger flow control on the spread of COVID-19. Let

$$W_{nm}^{new} = T_r \cdot W_{nm},$$

where W_{nm} is the passenger flow from the n -th patch to the m -th patch, and T_r represents the intensity of passenger flow control. The smaller the T_r , the greater the reduction in passenger flow.

There are two approaches for passenger flow control. One is to reduce the passenger flow for all provinces (global control in the mainland China), and the other is to control the flow only for high-risk local areas (local control, such as Hebei, Beijing, Heilongjiang, etc). Figure 8 shows that the reduction of local passenger flow and the reduction of passenger flow in all provinces have no significant difference on the overall pandemic transmission. Figure 9 shows that, in the areas where the infected population is erupting (such as Hebei Province), the greater intensity control of passenger flow, the more serious pandemic becomes. But, for low-risk areas (such as Jiangsu Province),

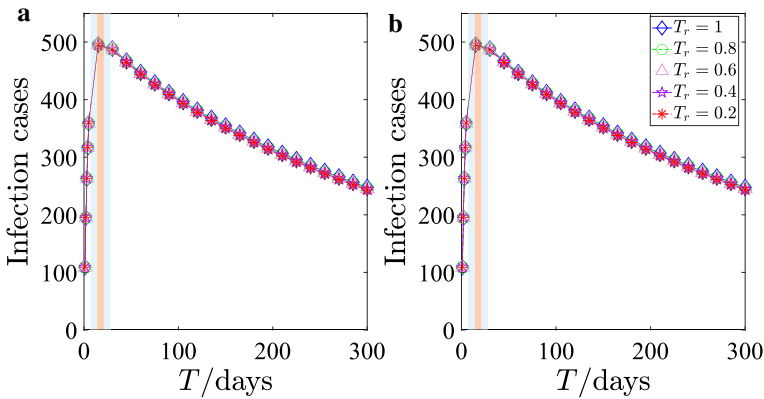


Fig. 8 Impact of T_r on COVID-19 transmission. **a** Global passenger flow control in China. **b** Local passenger flow control only in high-risk areas, such as in Hubei, Beijing, Heilongjiang. As we can see, **a** and **b** have no significant difference

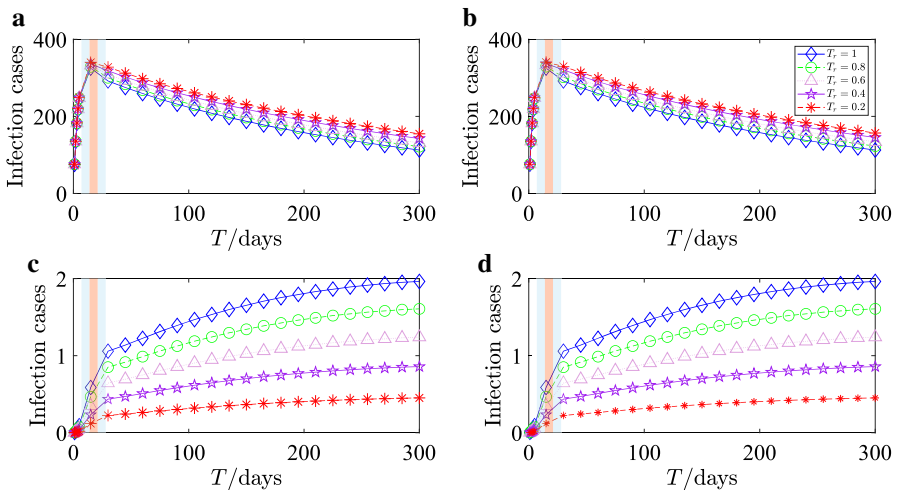


Fig. 9 Impact of T_r on COVID-19 transmission in high-risk areas and low-risk areas. **a** and **b** Represent global and local flow control in Hubei Province (high-risk area), respectively. **c** and **d** represent global and local flow control in Jiangsu Province (low-risk area), respectively

the greater the intensity of passenger flow control, the less likely it is to cause large-scale infections. The main reason for the above phenomenon is that the passenger flow control in the high-risk areas of the pandemic causes the more infected individuals to stay in high-risk areas, which renders the situation worse.

3.7 Vaccination Strategy

The Chinese government is now promoting vaccination. Here we assume the overall number of vaccines supplied in China is 1,000,000 per day. The number of vaccines

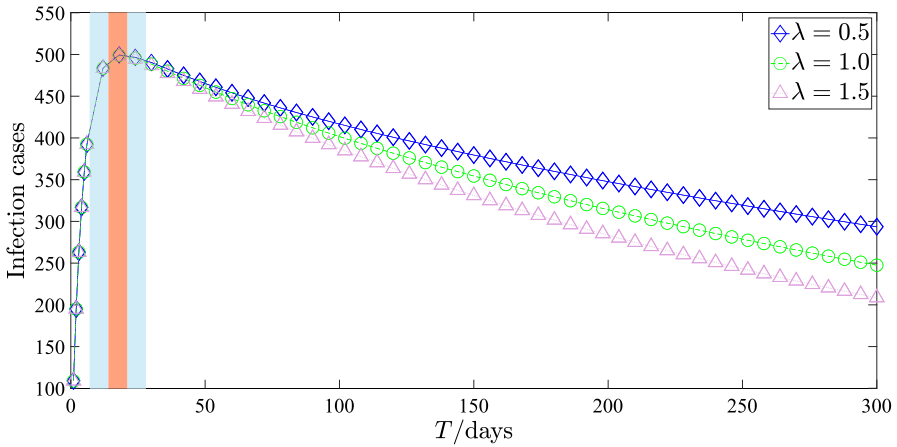


Fig. 10 The impact of vaccination number on COVID-19 transmission

distributed to each province is proportion to the population of the target region, which ensures the equal probability of each person being vaccinated. Let $N_{nv}^{new} = \lambda N_{nv}$. Then, and we discuss the impact of λ on the COVID-19 transmission. The result is shown in Fig. 10, which indicates that more vaccinated population can control the pandemic transmission.

Next, we explore the impact of the effectiveness v_e of the vaccine on COVID-19 transmission. The simulation results are presented in Fig. 11. We discover that during the early stages of pandemic, v_e does not have a significant impact on the pandemic transmission. However, in the process of remission, the stronger the effectiveness, the faster the remission of pandemic.

Finally, assuming that the immunity period is limited, we study its impact on COVID-19 transmission. The results are shown in Fig. 12, which implies that a longer immunity period is positive to the prevention of pandemic transmission.

4 Concluding Remarks

In this paper, a multiple patch coupled model based on the transportation network is established to explore transmission mechanism of COVID-19, under the combined effect of vaccination and NPIs in large-scale population migration. For the basic model, at least 61.38% of people need to be vaccinated to achieve the herd immunity. In the case of simultaneous implementation of vaccination and quarantine, it is necessary to ensure that the quarantine rate satisfies $p_2 > 38.74\%$ for preventing the disease spread further. By the sensitivity of \mathcal{R}_0 with variation of parameters, we find that the quarantine rate p_2 has the most significant impact on \mathcal{R}_0 . Therefore, before reaching herd immunity, a high-strength quarantine for newly infected cases is critical to prevent the spread of pandemic.

We investigate the impact of large-scale population migration during the CSF rush on the COVID-19 transmission. As for Chinese provinces with large-scale emigration,

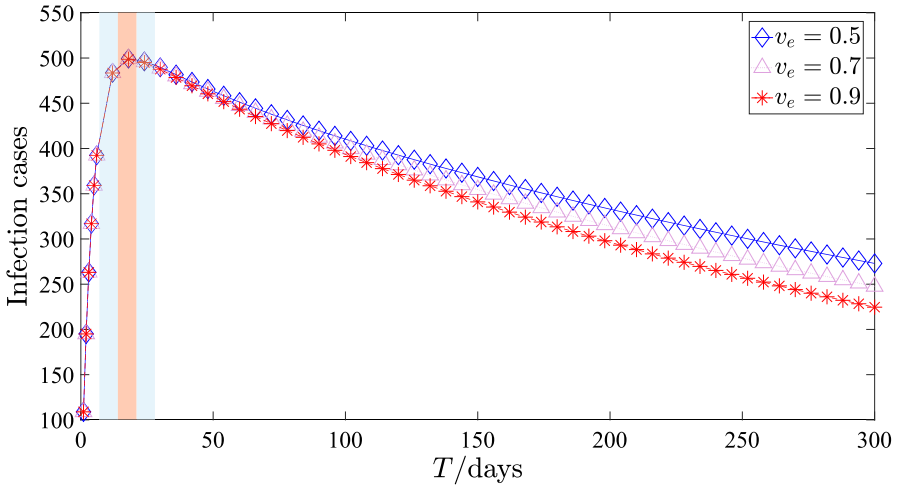


Fig. 11 The impact of vaccine effectiveness on COVID-19 transmission

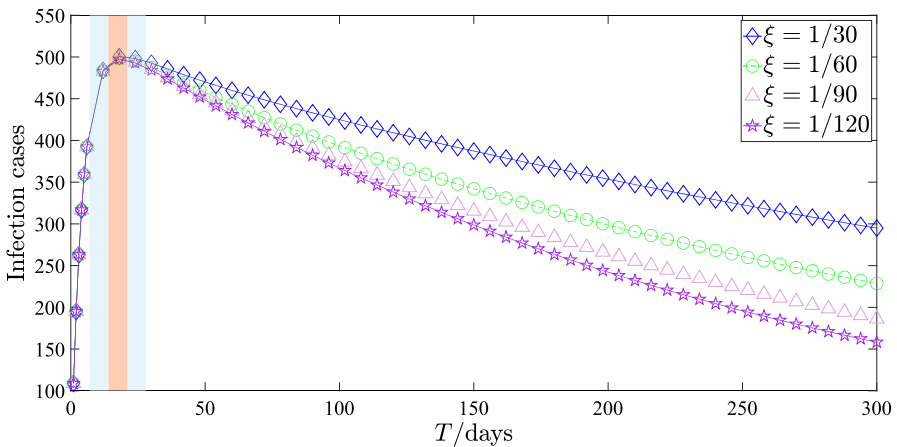


Fig. 12 The impact of immunity period on COVID-19 transmission

\mathcal{R}_0 decreases, whereas for the provinces with large-scale immigration, \mathcal{R}_0 increases. Furthermore, a comparison is made between the global and the local intervention of passage flow. Considering the overall pandemic situation in China, the evolutions of the local intervention and the overall intervention are basically the same. Therefore, the government only needs to control the population migration in high-risk areas. Meanwhile, numerical simulations show that the infectious diseases don't spread on a large scale under high-intensity population migration. The joint implementation of vaccines and quarantine ensures the controllability of the pandemic.

Effective vaccination has positive impact on prevention of pandemic transmission. We simulate the effect of vaccines number, the effectiveness, and the immune protection period on the pandemic transmission. When the number of vaccination increases,

the positive effect is more outstanding. The higher the effectiveness of the vaccine, the more significant the positive effect. Furthermore, the longer immune protection period can also have a better suppression effect on the pandemic spread.

Finally, our study only uses the simulated population migration data generated based on Baidu's migration rate data. In the future, if we are provided real population migration data, we can establish a model that performs a more realistic evaluation of vaccine injection and quarantine under large-scale population migration. Overall, we anticipate that, all the results presented in the paper could provide suggestions for policy makers on the prevention of COVID-19 transmission.

Acknowledgements W.Y. was supported by the STCSM (Grant Nos. 21511100200, 18ZR1404300). W.L. was supported by the National Natural Science Foundation of China (Grant No. 11925103), by the National Key R&D Program of China (Grant No. 2018YFC0116600), and by the STCSM (Grant Nos. 18DZ1201000, 19511101404, 19511132000).

Code Availability All MATLAB code used in this study are available on request from the corresponding author.

Conflict of interest All the authors declare no competing interests.

References

- Amato M, Werba JP, Frigerio B, Coggi D, Sansaro D, Ravani A, Ferrante P, Veglia F, Tremoli E, Baldassarre D (2020) Relationship between influenza vaccination coverage rate and COVID-19 outbreak: an Italian ecological study. *Vaccines* 8(3):535
- Auger P, Moussaoui A (2021) On the threshold of release of confinement in an epidemic seir model taking into account the protective effect of mask. *Bull Math Biol* 83(4):1–18
- Brockmann D, Helbing D (2013) The hidden geometry of complex, network-driven contagion phenomena. *Science* 342(6164):1337–1342
- Brown SM, Doom JR, Lechuga-Peña S, Watamura SE, Koppels T (2020) Stress and parenting during the global COVID-19 pandemic. *Child Abuse Negl* 110:104699
- Bubar KM, Reinholt K, Kissler SM, Lipsitch M, Cobey S, Grad YH, Larremore DB (2021) Model-informed COVID-19 vaccine prioritization strategies by age and serostatus. *Science* 371(6532):916–921
- Chang S, Pierson E, Koh PW, Gerardin J, Redbird B, Grusky D, Leskovec J (2021) Mobility network models of COVID-19 explain inequities and inform reopening. *Nature* 589(7840):82–87
- DeRoo SS, Pudalov NJ, Fu LY (2020) Planning for a COVID-19 vaccination program. *JAMA* 323(24):2458–2459
- Di Domenico L, Pullano G, Sabbatini CE, Boëlle PY, Colizza V (2021) Modelling safe protocols for reopening schools during the COVID-19 pandemic in France. *Nat Commun* 12(1):1–10
- Fang H, Wang L, Yang Y (2020) Human mobility restrictions and the spread of the novel coronavirus (2019-ncov) in China. *J Public Econ* 191:104272
- Gallagher ME, Sieben AJ, Nelson KN, Kraay AN, Lopman B, Handel A, Koelle K (2020) Considering indirect benefits is critical when evaluating sars-cov-2 vaccine candidates. medRxiv
- Gostin LO, Salmon DA (2020) The dual epidemics of COVID-19 and influenza: vaccine acceptance, coverage, and mandates. *JAMA* 324(4):335–336
- Guan D, Wang D, Hallegatte S, Davis SJ, Huo J, Li S, Bai Y, Lei T, Xue Q, Coffman D et al (2020) Global supply-chain effects of COVID-19 control measures. *Nat Hum Behav* 4(6):577–587
- Hou J, Hong J, Ji B, Dong B, Chen Y, Ward MP, Tu W, Jin Z, Hu J, Su Q et al (2021) Changed transmission epidemiology of COVID-19 at early stage: a nationwide population-based piecewise mathematical modelling study. *Travel Med Infect Dis* 39:101918
- Huang B, Wang J, Cai J, Yao S, Chan PKS, Tam THW, Hong YY, Ruktanonchai CW, Carioli A, Floyd JR et al (2021) Integrated vaccination and physical distancing interventions to prevent future COVID-19 waves in Chinese cities. *Nat Hum Behav* 5(6):695–705

- Ivorra B, Ferrández MR, Vela-Pérez M, Ramos A (2020) Mathematical modeling of the spread of the coronavirus disease 2019 (COVID-19) taking into account the undetected infections: the case of China. *Commun Nonlinear Sci Numer Simul* 88:105303
- Jacobsen KH (2020) Will COVID-19 generate global preparedness? *Lancet* 395(10229):1013–1014
- Jeyanathan M, Afkhami S, Smaili F, Miller MS, Lichty BD, Xing Z (2020) Immunological considerations for COVID-19 vaccine strategies. *Nat Rev Immunol* 20(10):615–632
- Kim JH, Marks F, Clemens JD (2021) Looking beyond COVID-19 vaccine phase 3 trials. *Nat Med* 27(2):205–211
- Kissler SM, Kishore N, Prabhu M, Goffman D, Beilin Y, Landau R, Gyamfi-Bannerman C, Bateman BT, Snyder J, Razavi AS et al (2020) Reductions in commuting mobility correlate with geographic differences in sars-cov-2 prevalence in New York city. *Nat Commun* 11(1):1–6
- Kraemer MU, Yang CH, Gutierrez B, Wu CH, Klein B, Pigott DM, Du Plessis L, Faria NR, Li R, Hanage WP et al (2020) The effect of human mobility and control measures on the COVID-19 epidemic in China. *Science* 368(6490):493–497
- Lai S, Ruktanonchai NW, Zhou L, Prosper O, Luo W, Floyd JR, Wesolowski A, Santillana M, Zhang C, Du X et al (2020) Effect of non-pharmaceutical interventions to contain COVID-19 in China. *Nature* 585(7825):410–413
- Lau H, Khosrawipour V, Kocbach P, Mikolajczyk A, Schubert J, Bania J, Khosrawipour T (2020) The positive impact of lockdown in Wuhan on containing the COVID-19 outbreak in China. *J Travel Med* 27(3):taaa037
- Li HL, Jecker NS, Chung RYN (2020a) Reopening economies during the COVID-19 pandemic: reasoning about value tradeoffs. *Am J Bioeth* 20(7):136–138
- Li Q, Guan X, Wu P, Wang X, Zhou L, Tong Y, Ren R, Leung KS, Lau EH, Wong JY et al (2020) Early transmission dynamics in Wuhan, China, of novel coronavirus-infected pneumonia. *N Engl J Med* 382(13):1199–1207
- Lipsitch M, Dean NE (2020) Understanding COVID-19 vaccine efficacy. *Science* 370(6518):763–765
- Liu J, Hao J, Sun Y, Shi Z (2021) Network analysis of population flow among major cities and its influence on COVID-19 transmission in China. *Cities* 112:103138
- Medlock J, Galvani AP (2009) Optimizing influenza vaccine distribution. *Science* 325(5948):1705–1708
- Mu X, Yeh AGO, Zhang X (2020) The interplay of spatial spread of COVID-19 and human mobility in the urban system of China during the Chinese new year. *Environ Plan B Urban Anal City Sci* 48(6487):2399808320954211
- Nishi A, Dewey G, Endo A, Neman S, Iwamoto SK, Ni MY, Tsugawa Y, Iosifidis G, Smith JD, Young SD (2020) Network interventions for managing the COVID-19 pandemic and sustaining economy. *Proc Natl Acad Sci* 117(48):30285–30294
- Pan C (2018) The role of time delays in dynamical eco- and bio-systems and in prediction of system evolutions. Ph.D. thesis, Fudan University
- Perkins TA, España G (2020) Optimal control of the COVID-19 pandemic with non-pharmaceutical interventions. *Bull Math Biol* 82(9):1–24
- Pujari BS, Shekatkar SM (2020) Multi-city modeling of epidemics using spatial networks: application to 2019-ncov (COVID-19) coronavirus in India. *Medrxiv*
- Sheikh A, Sheikh A, Sheikh Z, Dhami S (2020) Reopening schools after the COVID-19 lockdown. *J Glob Health* 10(1):010376
- Shen M, Zu J, Fairley CK, Pagán JA, An L, Du Z, Guo Y, Rong L, Xiao Y, Zhuang G et al (2021) Projected COVID-19 epidemic in the united states in the context of the effectiveness of a potential vaccine and implications for social distancing and face mask use. *Vaccine* 39(16):2295–2302
- Thompson MG, Burgess JL, Naleway AL, Tyner HL, Yoon SK, Meece J, Olsho LE, Caban-Martinez AJ, Fowlkes A, Lutrick K et al (2021) Interim estimates of vaccine effectiveness of bnt162b2 and mrna-1273 COVID-19 vaccines in preventing sars-cov-2 infection among health care personnel, first responders, and other essential and frontline workers—eight us locations, December 2020–March 2021. *Morb Mortal Wkly Rep* 70(13):495
- Van den Driessche P, Watmough J (2002) Reproduction numbers and sub-threshold endemic equilibria for compartmental models of disease transmission. *Math Biosci* 180(1–2):29–48
- Wesolowski A, Eagle N, Tatem AJ, Smith DL, Noor AM, Snow RW, Buckee CO (2012) Quantifying the impact of human mobility on malaria. *Science* 338(6104):267–270

Zhang J, Litvinova M, Liang Y, Wang Y, Wang W, Zhao S, Wu Q, Merler S, Viboud C, Vespignani A et al (2020) Changes in contact patterns shape the dynamics of the COVID-19 outbreak in China. *Science* 368(6498):1481–1486

Publisher's Note Springer Nature remains neutral with regard to jurisdictional claims in published maps and institutional affiliations.

Authors and Affiliations

Yukun Zou^{1,2} · Wei Yang¹  · Junjie Lai^{1,2} · Jiawen Hou^{1,2} · Wei Lin^{1,3,4}

✉ Wei Yang
yangwei@fudan.edu.cn

Yukun Zou
ygzou19@fudan.edu.cn

Wei Lin
wlin@fudan.edu.cn

- ¹ Research Institute of Intelligent Complex Systems, Fudan University, Shanghai 200433, China
- ² Institute of Science and Technology for Brain-Inspired Intelligence, Fudan University, Shanghai 200433, China
- ³ School of Mathematical Sciences, SCMS, and SCAM, Fudan University, Shanghai 200433, China
- ⁴ State Key Laboratory of Medical Neurobiology, and MOE Frontiers Center for Brain Science, Institutes of Brain Science, Fudan University, Shanghai 200032, China